ARTICLE

Hapten design to prepare monoclonal antibodies and establishment of immunoassay for direct screening of oxamichydrazide in chicken, the metabolite of nifuraldezone

Ghulam Mujtaba Mari[1], Weilin Wu[2], Aisha Talpur[1], Jan Muhammad Shah[1], Saqib Ali[1], Faiz Khand[3], Erum Bughio[4], Abdul Samad[5], Zhanhui Wang[2] and Sergei A. Eremin[6*]

Abstract

In this study, two novel haptens of oxamichydrazide (OXZ), the metabolite of nifuraldezone, were designed and synthesized by derivatization with ethyl-4-bromobutanoate and ethyl-2-bromoacetate for the first time. The rationality of the haptens was enlightened by conformational alignment and electronic evaluations based on computional chemistry. The synthesized haptens were efficient in generating antibody response to OXZ. A monoclonal antibody (mAb) named 2D9 with high affinity was obtained and used to establish an indirect competitive enzyme-linked immuno-sorbent assay (icELISA) for the direct determination of OXZ in chicken samples without the need for derivatization step. Under optimum conditions, the developed icELISA showed an IC_{50} value of 0.66 ng mL^{-1}, and limit of detection of 0.11 µg kg^{-1} in chicken. The average recoveries were found to be 80.4–91.3% with a coefficient of variation less than 9.0%. In conclusion, we have successfully designened haptens, prepared mAbs and developed an immunoassay for the direct determination of OXZ in chicken samples without the need for a derivatization step for the first time. This provides a potentially rapid, accurate, and sensitive screening tool for nifuraldezone residue in animal-derived food.

Keywords Nifuraldezone, Oxamichydrazide, Hapten design, Monoclonal antibody, icELISA, Direct determination

*Correspondence:
Sergei A. Eremin
eremin_sergei@hotmail.com
[1] Department of Veterinary Pharmacology and Toxicology, Faculty of Bio-Sciences, Shaheed Benazir Bhutto University of Veterinary and Animal Sciences, Sakrand 67210, Pakistan
[2] National Key Laboratory of Veterinary Public Health Security, Beijing Key Laboratory of Detection Technology for Animal-Derived Food Safety, College of Veterinary Medicine, China Agricultural University, Beijing 100193, China
[3] Department of Veterinary Surgery and Obstructers, Faculty of Veterinary Sciences, Shaheed Benazir Bhutto University of Veterinary and Animal Sciences, Sakrand 67210, Pakistan
[4] Department of Poultry Production, Faculty of Animal Production and Technology, Shaheed Benazir Bhutto University of Veterinary and Animal Sciences, Sakrand 67210, Pakistan
[5] Department of Dairy Technology, Faculty of Animal Production and Technology, Shaheed Benazir Bhutto University of Veterinary and Animal Sciences, Sakrand 67210, Pakistan
[6] Department of Chemistry, M.V. Lomonosov Moscow State University, 119991 Moscow, Russia

Mari *et al. One Health Advances*   (2023) 1:6

Page 2 of 12

Introduction

Nitrofurans belong to a group of synthetic broad-spectrum antibacterial agents, all of which contain a 5-nitrofuran ring [1]. Due to their high effectiveness, easy accessibility, and relatively cheap production, nitrofurans became popular all over the world as veterinary drugs and were frequently used to treat gastrointestinal, and dermatological salmonellosis infections in poultry, cattle, swine, and fish [2]. However, due to their carcinogenic and mutagenic effects on human health, the European Union restricted the use of nitrofurans in food-producing animals by Commission Regulation No 1442/95 [3]. Later, another Commission Decision (2003/181/EC) was issued with the minimum required performance limits (MRPLs) for nitrofurans of 1.0 μg kg^{-1} in aquaculture products and poultry meat [4]. Recently, the Commission Decision 2019/1871 established Reference Point for Action (RPA) for nitrofuran metabolites at 0.5 μg kg^{-1} and applied from 28 November 2022 [5]. This requires the development of more sensitive analytical method for the detecting of nitrofurans residues. It has been discovered that parent nitrofurans have a short half-life in vivo and could not be identified in tissue or blood following slaughter [6–8]. Further research confirmed that nitrofurans metabolize quickly, but their metabolites bind to tissue proteins stably, persisting in animal tissues following the withdrawal of treatment [9, 10]. Therefore, the metabolites of nitrofurans are generally utilized as markers for nitrofurans residues in foods.

It was previously thought that direct detection of these metabolites was impractical due to their small size, and thus, derivatization of these metabolites with derivative reagents such as 2-nitrobenzaldehyde (2-NBA) was compulsory to make larger nitrophenyl (NP) derivatives earlier to the determination, enabling efficient results in both antibody-based assays [11–13] such as enzyme-linked immunosorbent assay (ELISA), lateral flow immunoassay, and instrument-based methods [9, 14, 15] like high-performance liquid chromatography-tandem mass spectrometry (HPLC–MS/MS) [16]. However, derivatization was often accompanied by time waste and complex operations. Actually, direct detection of the metabolite from food samples without derivatization can be achieved if the high-affinity antibodies to metabolites are obtained. To our best knowledge, few reports have surfaced on the successful development of specific antibodies and corresponding immunoassays for directly detecting nitrofuran metabolites [17, 18].

Nifuraldezone (NAZ) is a member of nitrofuran drugs, probably used to treat diseases or as a growth promoter in poultry and aquaculture. Due to serious threats to human health, most countries worldwide, including the EU, China and the USA have banned the use of nitrofurans in all food-producing animals [3, 19, 20]. However, they are still illegally prepared and issued for practice in many countries worldwide, particularly in developing countries due to cost-effectiveness [21]. To safeguard food safety and human health, it is essential to establish easy, high-throughput screening methods for the direct detection of NAZ metabolites, considering time costs, oxamichydrazide (OXZ) [22, 23] in animal-origin foods [16, 24]. To date, neither instrument-based nor antibody-based analytical techniques have been established to detect OXZ. Immunoassays are recommended as the first-rate choice in the rapid screening of drug residues in food samples due to advantages such as user-friendly manipulation, high sensitivity and specificity. For immunoassay development, the antibody plays a critical role in the sensitivity and specificity of methods. Hapten rational design has been regarded as the most important factor in the generation of desired antibodies in terms of affinity and specificity. To obtain one required antibody to target analytes, the hapten should be rationally designed to mimic the target to a great extent. In this study, one new approach is brought forward in designing and synthesizing two novel haptens of OXZ with different derivative reagents as spacer arms to get desired outcomes. The rationality of these novel haptens was evaluated by computational chemistry. Followed by antigen preparation and immunization, highly-affinity monoclonal antibodies (mAbs) were achieved. These mAbs were then used to develop icELISA to detect OXZ directly in chicken tissues.

Results and discussions

Hapten design, synthesis and conjugates preparation

The objective of the current study was to prepare high-affinity mAbs to OXZ, with the expectation of developing an immunoassay without the need for derivatization. The significance of hapten design for small molecules cannot be undervalued, as it plays a vital role in the resulting antibody's affinity and specificity. One of the optimal criteria for hapten design is that it should mimic the target analyte as much as possible in relation to size, steric conformation, electronic properties, and hydrophobicity [25]. Due to their much smaller molecular size than proteins, the OXZ epitope, containing the amino active group, is easily shielded when coupled directly with the carrier protein. This ultimately fails to stimulate an OXZ-specific antibody response. Therefore, a derivative agent should be introduced as a spacer arm to support the epitope away from the protein at a proper distance and maximize the exposure of OXZ to the immune system. Generally, immunogenicity is positively correlated with molecular size and structural complexity. In the case of OXZ haptens, it is easily conceivable that the linear

Mari *et al. One Health Advances*   (2023) 1:6

Page 3 of 12

aliphatic chain-contained spacer arms have a limited increase in antigenicity because of their small and simple structure; On the other hand, the spacer arms containing a more complex and rigid benzene ring may be beneficial in stimulating a strong immune response. However, a complex spacer arm of a hapten may induce a non-specific antibody response and result in a low-affinity antibody to the target analyte. Considering that 2-NBA is frequently used in the pretreatment of OXZ to form NPOXZ, two OXZ haptens were designed with rigid benzene ring-contained spacer arms, as shown in Scheme 1. The structures of these OXZ haptens in the current study are expected to provoke a high-affinity and specific antibody response. Specially, to obtain high-affinity antibodies to OXZ, not just NPOXZ, the two haptens were decorated with different lengths of fatty chains and rigid benzene ending with a carboxyl group. Previous research has shown that haptens containing spacer arms of four to six carbon lengths were prone to yielding high-performance antibodies due to their ability to appropriately sustain epitopes [26, 27]. As can be seen in Scheme 1, Hapten B has a shorter carbon chain than Hapten A, making insignificant non-OXZ structures less exposed in Hapten B than in Hapten A under the shielding action from proteins. Moreover, haptens with a longer chain than Hapten A are possibly inclined to bend [28], thus exposing non-OXZ structures more easily. Since, both haptens provide a high possibility of inducing an antibody response to OXZ, the rationality and feasibility of the designed haptens were further evaluated in conformational and electronic studies by computational chemistry.

Based on the calculated lowest energy conformation, OXZ, Hapten A, and B were aligned. The alignments in Fig. 1A indicated that the OXZ moiety of haptens overlapped well with the target molecule OXZ, demonstrating that the insertion of spacer arms at the N29 position barely influenced the conformational OXZ feature of the haptens. In addition to steric conformation, the electronic property is another critical factor in the antigenicity of a hapten. The Mulliken charges on each heavy atom of OXZ and the haptens were calculated, extracted, and compared in Fig. 1B. It is easy to observe that OXZ and haptens had high similarity in atom charges at the N31/C33/C35/O36 position, with a difference less than 0.1 a.u. Although the introduced spacer arms resulted in the variation of atomic charges distribution at N29/N30/O34 position of OXZ moiety without exceeding 0.2 a.u., it can be suggested that the difference may have limited influence on the recognition of antibody and analyte. These results showed the two designed haptens well mimicked the target OXZ in conformational and electronic characters, determining that the designed haptens of the

current study could be synthesized and employed to produce antibodies to OXZ.

The two haptens were synthesized according to Scheme 1. Hapten A used ethyl 4-bromobutanoate, while Hapten B used ethyl-2-bromoacetate as spacer arms. In addition, the derivative of NPOXZ was synthesized using 2-NBA. Structural characterizations of haptens and NPOXZ were carried out using mass spectrum and NMR analysis, as shown in Figure S1 and S2 of the *Supporting Information*. Activation of the haptens with NHS and DCC was followed by successful conjugation to carrier proteins, and the resulting conjugates to carrier proteins showed an apparent shift in the highest peak position compared to the control protein, as shown in Figure S3. The molar coupling ratios of haptens to BSA were calculated to be 7.98:1 (Hapten A-BSA) and 7.05:1 (Hapten B-BSA), respectively.

Antiserum Analysis and mAb Generation

The two hapten–KLH conjugates were used to inoculate a group of five mice individually three times at three-week intervals. After the third immunization, antisera were collected and their antibody titers and IC_{50} values for OXZ and NPOXZ were determined based on both homologous and heterologous ELISA, respectively. The lower IC_{50} values and higher antibody titers suggest a stronger specific immune response to target analytes. The parameters of mice antisera were detailed in Table 1, indicating that all mice receiving two immunogens showed significant specific antibody response with antibody titers all exceeding 10,000. Further validation was provided that the Hapten B with a shorter spacer arm enhanced antigenicity and thus showed slightly better antibody titers on both homologous and heterologous icELISA, respectively. In the field of immunoassay for small molecules, the IC_{50} value is a more critical parameter that deserves our attention. The results in Table 1 revealed that all antisera showed obvious recognition with OXZ and NPOXZ. Specifically, all antisera recognized NPOXZ better with lower IC_{50} values than OXZ, which was possibly due to the influence of the nitrobenzene group in the haptens. It is worth noting that the IC_{50} values from heterologous icELISA were all lower than those from homologous icELISA, whether antisera were from the Hapten A or Hapten B. Specifically, the antisera obtained from Hapten A-KLH offered IC_{50} values ranging from 88.1–211.4 ng mL^{-1} for OXZ with average values of 149.2 ng mL^{-1} and 47.6–96.6 ng mL^{-1} for NPOXZ with average values of 74.64 ng mL^{-1} based on heterologous antigen Hapten B-BSA. Likewise, antisera from Hapten B-KLH exhibited IC_{50} values ranging from 28.1–156.2 ng mL^{-1} for OXZ with average values of 93.22 ng mL^{-1} and 12.4–68.3 ng mL^{-1} for NPOXZ with
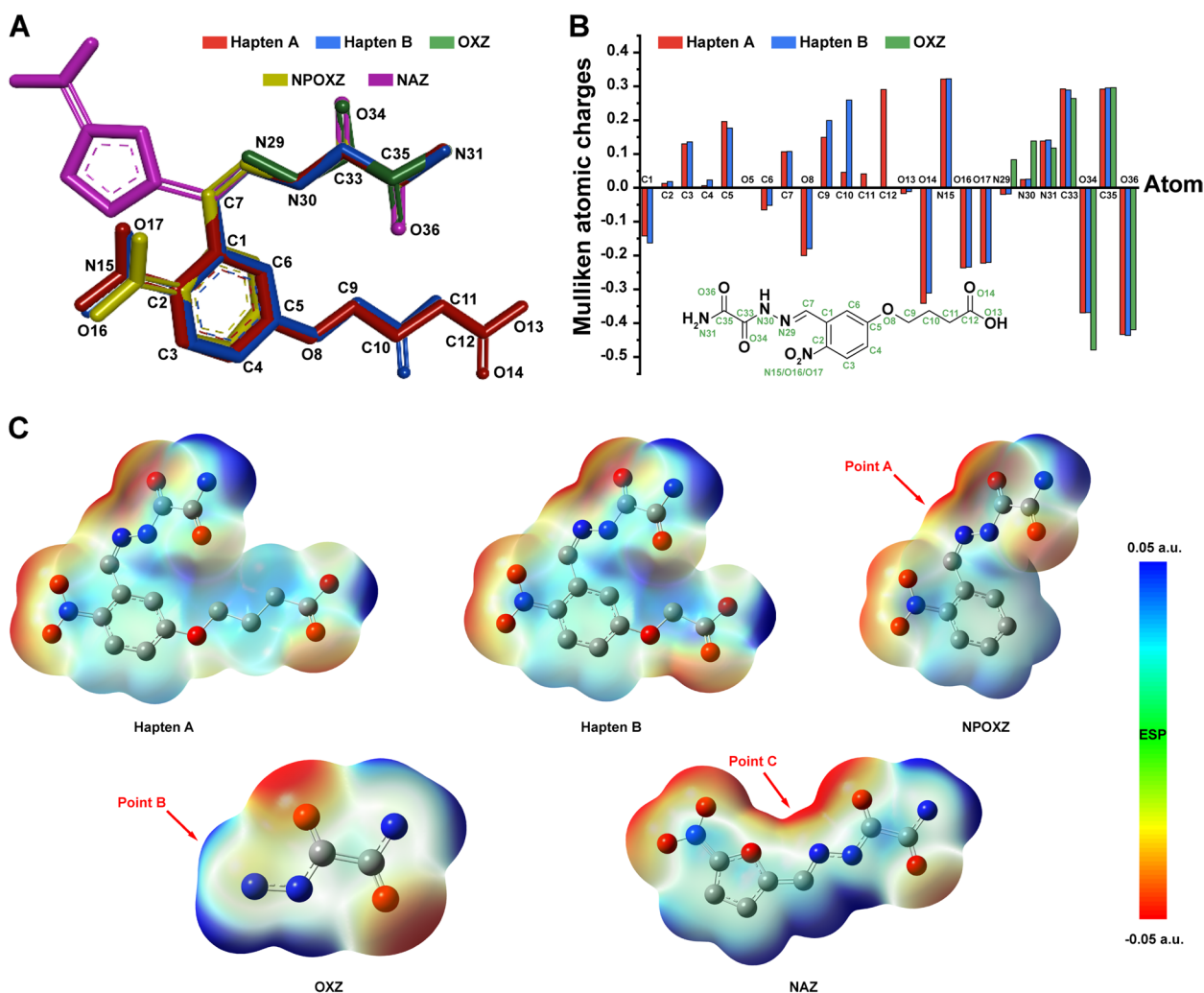
Fig. 1 Computational chemistry results, (**A**) the alignment of Hapten A, Hapten B, OXZ, NPOXZ and NAZ. (**B**) calculated partial atomic charges of Hapten A, Hapten B and OXZ. (**C**) ESP of Hapten A, Hapten B, NPOXZ, OXZ and NAZ. The positive ESP sections are specified in blue, and the negative sections in red

average values of 44.78 ng mL^{-1} based on heterologous assays. As expected, the average values of antibody titers and the IC$_{50}$ from Hapten B-KLH were superior to those from Hapten A-KLH under heterologous pairs, implying that the ethyl-2-bromoacetate used as a derivative reagent was more suitable for OXZ hapten design owing probably to the better stability and less spacer binding effects of the shorter-chain haptens. Especially, the anti-sera from Hapten B-2#, when paired with Hapten A-BSA as the coating antigen, yielded the best IC$_{50}$ values of 28.1 and 12.4 ng mL^{-1} for OXZ and NPOXZ, respectively.

The best mouse from each hapten was sacrificed for mAbs preparation, i.e. mouse No. 2# from Hapten B and No. 5# from Hapten A. Finally, a total of two hybridomas, named 2D9 and 2B6, were obtained. These mAbs were prepared as ascetic fluids without further purification and characterized. After optimization of concentrations using the checkerboard method, it can be observed in Table 1 and S1 the optimum dilutions of both mAbs were 1/81000 and improved by more than 3 times in comparison with the corresponding anti-sera when furnishing OD$_{max}$ between 1.5 and 2.0 at the identical coating antigen, while the IC$_{50}$ of the ascites improved by more than 40 times. Particularly, the outstandingly low IC$_{50}$ values offered by the 2D9 could meet the high detectability levels required for OXZ monitoring. Thus, mAb 2D9 and coating antigen Hapten A-BSA were paired for subsequent experiments.

Mari *et al. One Health Advances*   (2023) 1:6

Page 5 of 12

Table 1 Characterization of mice antisera and mAbs with homologous and heterologous coating antigens

Haptens/Mice#	Coating antigen Hapten A-BSA[a]			Coating antigen Hapten B-BSA		
	Antibody titers	IC_{50} for OXZ (ng mL^{-1})	IC_{50} for NPOXZ (ng mL^{-1})	Antibody titers	IC_{50} for OXZ (ng mL^{-1})	IC_{50} for NPOXZ (ng mL^{-1})
Hapten-A-1#	1/15000	375.5	133.2	1/10000	121.2	89.3
Hapten-A-2#	1/15000	256.3	143.5	1/12000	189.7	96.6
Hapten-A-3#	1/14000	461.5	122.7	1/14000	211.4	71.2
Hapten-A-4#	1/13000	353.9	126.1	1/10000	135.2	68.5
Hapten-A-5#[b]	**1/18000**	**519.1**	**189.3**	**1/16000**	**88.1**	**47.6**
Average values[c]	1/15000	393.26	142.96	1/12400	149.12	74.64
mAb 2B6	1/81000	1.89	1.46	1/81000	1.42	0.95
Hapten-B-1#	1/20000	50.5	31.3	1/11000	278.3	148.9
Hapten-B-2#	**1/27000**	**28.1**	**12.4**	1/20000	158.3	112.6
Hapten-B-3#	1/20000	98.2	68.3	1/19000	198.6	125.8
Hapten-B-4#	1/20000	156.2	65.6	1/15000	176.5	123.2
Hapten-B-5#	1/20000	133.1	46.3	1/15000	146.4	126.1
Average values	1/21400	93.22	44.78	1/16000	191.62	127.32
mAb 2D9	1/81000	0.66	0.21	1/81000	0.98	0.61

[a] The concentration of Hapten A-BSA and Hapten B-BSA for antisera evaluation was 0.74 and 0.62 mg L^{-1}, and the concentration for mAbs evaluation was 0.5 and 0.44 mg L^{-1}, respectively

[b] The mice with the highest affinity in each group were bold

[c] Average values of the antisera characterization parameters in each group

Establishment and Optimization of icELISA for OXZ

Antigen–antibody reactions are susceptible to some physicochemical parameters, which in turn compromises the performance of icELISA [29]. Accordingly, some parameters were optimized in this study for better icELISA performances, including the incubation procedure (4°C for 24 h, 25°C for 1 h, 37°C for 30 min) in the competition step, pH values (5.5, 6.0, 7.0, 7.4, and 8.0 of PBS), and ionic strength (0.0, 0.1, 0.5 and 1.0 mol L^{-1} of NaCl concentrations in PBS). In this
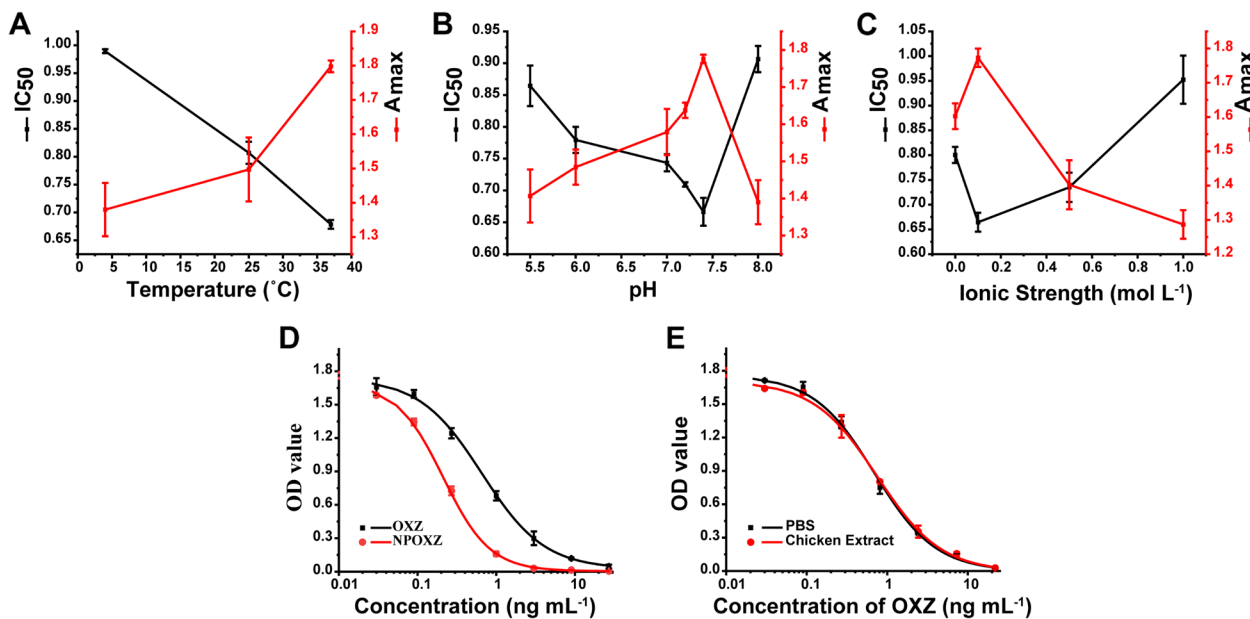

Fig. 2 The influence of (**A**) Temperature (°C), (**B**) pH, and (**C**) ionic strength concentrations on the performance of icELISA for OXZ ($n=3$). (**D**) The icELISA standard curves for OXZ and NPOXZ using the Hapten A-BSA as coating antigen based on mAb 2D9. (**E**) The icELISA calibration curves for evaluation of the chicken extract matrix effect to OXZ determination ($n=3$)

Mari *et al. One Health Advances*   (2023) 1:6

Page 6 of 12

Table 2 Cross Reactivity (CR) of mAb 2D9-based icELISA against various nitrofuran drugs and metabolite derivatives

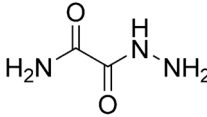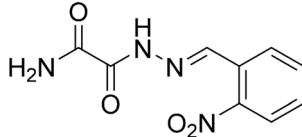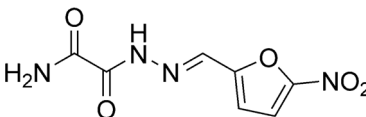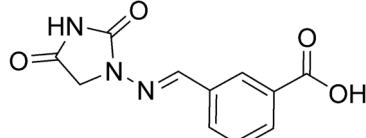| Compounds	Structure	CR (%)	IC$_{50}$ (ng mL^{-1})
OXZ		100	0.66
NPOXZ		314.28	0.21
NAZ		9.55	6.91
CPAHD		<0.06	>1000
CPAOZ		<0.06	>1000
CPAMOZ		<0.06	>1000
Nitrovin		<0.06	>1000
Nifuroxazide		<0.06	>1000
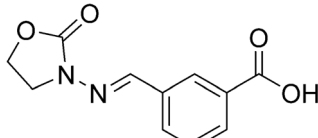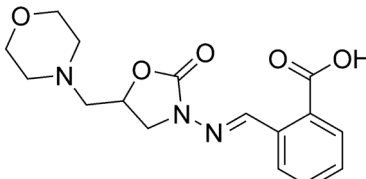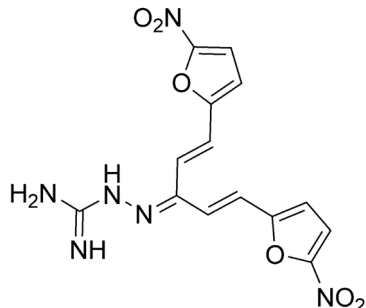
Mari *et al. One Health Advances* (2023) 1:6

Page 7 of 12
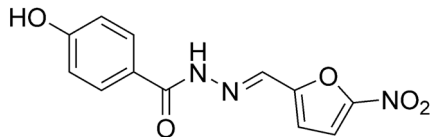
Table 3 Recovery and coefficient of variation (CV) of the icELISA for OXZ in chicken samples ($n = 5$)[a]

Matrix	spiked (µg kg^{-1})	found (µg kg^{-1})	recoveries (%)	intra-assay CV[b] (%)	inter-assay CV (%)	LOD (µg kg^{-1})
Chicken	0.5	0.42	84.5	8.6	8.9	0.11
	1.0	0.91	91.3	8.4	8.1	
	2.5	2.01	80.4	8.8	8.2	

[a] The value represents the average of five replicates

[b] CV is defined as the ratio of standard deviation to average
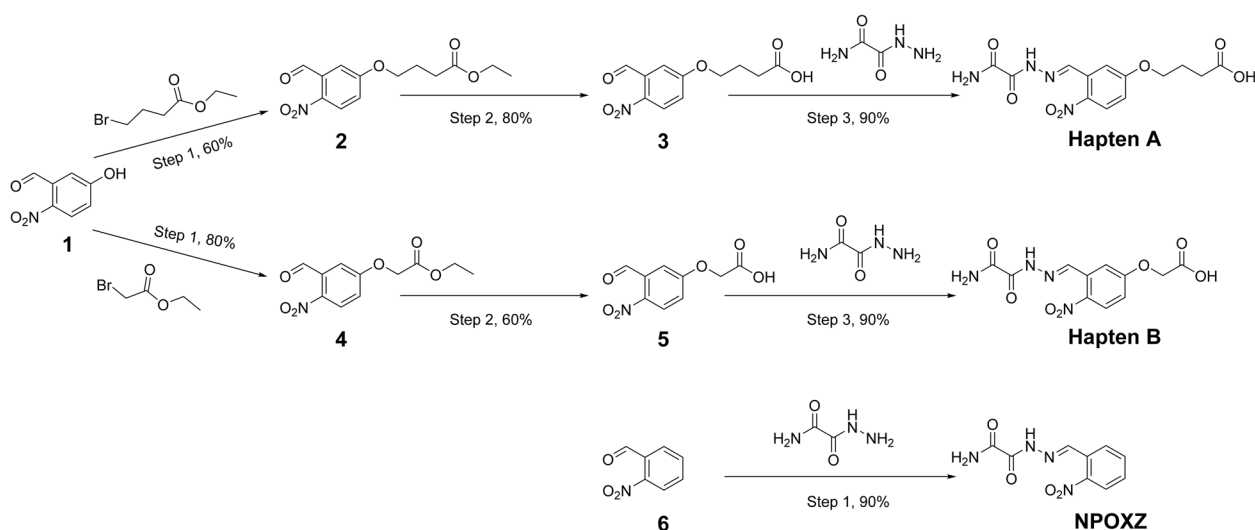
Scheme 1 OXZ haptens and NPOXZ synthetic routes

icELISA, the ability of mAb to react with coating antigens (represented by A_{max}) and the OXZ to compete with antigens for mAb (represented by IC_{50}) were used to accurately quantify these effects [30]. The highest A_{max} and lowest IC_{50} value, showed higher sensitivity of the icELISA. It can be observed in Fig. 2A, the A_{max} varied with temperature and achieved the highest value at 37°C, while, the A_{max} reached the maximum at pH 7.4 with the lowest IC_{50} value as revealed in Fig. 2B. Furthermore, the A_{max} declined more slowly in acidic than in alkaline conditions, suggesting that the mAb 2D9 was relatively more resistant to acids. In Fig. 2C, the optimum concentration of NaCl was recognized with 0.1 mol L^{-1}. Following the adoption of optimum conditions, i.e., 37°C for 30 min and PBS buffer at pH 7.4 with NaCl concentration of 0.1 mol L^{-1}, the standard curve of the icELISA for OXZ/NPOXZ was established as in Fig. 2D. The IC_{50} values of the developed ELISA for OXZ and NPOXZ were 0.66 and 0.21 ng mL^{-1}, respectively.

The specificity of the icELISA was assessed by substituting seven analogues, including nitrofurans (NAZ,

nitrovin, and nifuroxazide), and metabolite derivatives of nitrofurans (NPOXZ, CPAHD, CPAOZ, CPAMOZ). As shown in Table 2, the high CR for NPOXZ was expected, with a value of 314.28%, indicating the feasibility of simultaneous detection of OXZ and NPOXZ, while the low CR for the NAZ parent drug was 9.55%. The CRs for the other analogues were all below 0.06% due to their totally different structures. The significant difference in the ability of mAb 2D9 to recognize OXZ, NPOXZ, and NAZ drew our attention. However, two-dimensional structure analysis could not decipher the recognition profiles of mAb. Therefore, we further investigated the possible recognition mechanism of mAb from conformational and electronic aspects. As noted in Table 2, mAb 2D9 had the highest affinity to NPOXZ with an IC_{50} of 0.21 ng mL^{-1}. This can be explained by the best overlay resemblance of NPOXZ to Hapten B (Fig. 1A). When Hapten B-KLH (composed of NPOXZ, acetic acid, and protein) was used as the immunogen, it was speculated that the NPOXZ moiety served as the epitope to elicit antibodies, while the acetic acid served simply as the linker between NPOXZ and proteins. Therefore, the

Mari *et al. One Health Advances*   (2023) 1:6

Page 8 of 12

resulting mAb 2D9 displayed the best recognition ability towards NPOXZ with the lowest IC_{50} values. Further, a comprehensive explanation of the CR difference was provided in the ESP analysis. The ESP displays the potential energy of a proton placed near a molecule. Blue areas represent repulsive potential energy, while red areas represent attractive potential energy for a proton on the molecule. The ESP of OXZ, NPOXZ, and NAZ were calculated and visualized in Fig. 1C. Point A (N29 position) of NPOXZ possessed reasonable electronegativity. However, in the absence of the 1-methyl-2-nitrobenzene moiety, the strong positive electricity displayed at Point B (N29 position) of OXZ resulted in a threefold poorer recognition ability of mAb 2D9-OXZ. Compared with NPOXZ, NAZ contained the furan ring as an alternative to the benzene ring, and it came with stronger electronegativity at the corresponding Point C of NAZ and dissatisfactory conformation matching due to the introduction of an oxygen atom, resulting in a surprisingly 30-fold decrease in the recognition ability of mAb 2D9-NAZ than NPOXZ.

Matrix Effects and Recovery

The matrix effect of food samples may hinder the accurate quantification of the targeted analyte. In order to increase the enrichment of targets and reduce the matrix effect, pretreatment and clean-up are commonly required. In this study, sample extracts was collected following the pretreatment procedure of solvent extraction with ethyl acetate and degreasing. To evaluate the matrix effect, the standard curve of icELISA in PBS for OXZ was compared with that in the extract from chicken samples. Figure 2E shows that the matrix effect of chicken after pretreatment procedure had negligible interference with the performance of the icELISA, indicating that the pretreatment procedure was acceptable. The developed icELISA for OXZ exhibited the LOD and detection range of 0.11 μg kg^{-1} and 0.26–3.44 μg kg^{-1} in chicken. It is noteworthy that the developed icELISA with low LOD of OXZ was sensitive enough to directly detect OXZ in chicken without burdensome derivatization and provided superior or comparable sensitivity compared to reported immunoassays for the direct detection of other nitrofuran metabolites [17, 18]. To assess the accuracy of the developed icELISA, a recovery study for OXZ from negative chicken at three spiked concentrations (0.5, 1.0, and 2.5 μg kg^{-1}) was conducted. The mean recovery values were in the range of 80.4–91.3%, with the coefficient of variation (CV) values lower than 8.9% (Table 3). These findings indicated that the proposed mAb 2D9-based icELISA, with high sensitivity, specificity, accuracy, and precision, is ideally suited as

a screening method for OXZ directly from chicken tissues without the need for a derivatization step.

In summary, two new OXZ haptens were designed, synthesized and validated using computational chemistry and animal immunization. Results indicate that the mAbs to OXZ were prepared for the first time with an IC_{50} value of 0.66 ng mL^{-1}. Furthermore, mAb 2D9-based icELISA was established and proved to be highly sensitive in detecting OXZ without extra derivatization, with a LOD of 0.11 μg kg^{-1} in chicken, meeting the residue control requirement for OXZ.

Supporting information

The supporting information, including the buffer solutions, the structures and mass spectra and ^{1}HNMR spectra of haptens and NPOXZ, the figures of MALDI-TOF−MS analysis of carrier protein and the conjugates, and the parameters of the two mAbs derived from Hapten A and Hapten B pairing with Hapten A-BSA, Hapten B-BSA, as coating antigen for sensitivity evaluation, can be found in Supporting information section.

Materials and methods

Materials and reagents

NAZ was obtained from Witega laboratorien Berlin-Adlershof GmbH (Berlin, Germany). Oxamichydrazide, 5-hydroxy-2-nitrobenzaldehyde (NP), ethyl 4-bromobutanoate and ethyl 2-bromoacetate were obtained from TCI (Shanghai, China). Bovine serum albumin (BSA), Keyhole limpet hemocyanin (KLH), Freund's complete and incomplete adjuvant, hypoxanthine aminopterin thymidine (HAT), hypoxanthine thymidine (HT), poly ethylene glycol (PEG) 1500, and fetal bovine serum (FBS) were acquired from Sigma-Aldrich (St. Louis, MO, USA). N, N-dicyclohexylcarbodiimide (DCC), 3,3,5,5-Tetramethylbenzidine (TMB) and N-hydroxysuccinimide (NHS), were provided by Aladdin Reagent (Shanghai, China). Horseradish peroxidase (HRP) conjugated goat anti-mouse IgG antibody was procured from Jackson Immuno Research Laboratories (West Grove, PA, USA). Commonly used reagents, such as sodium chloride (NaCl), and dimethylformamide (DMF) were purchased from Sinopharm Chemical Reagent (Beijing, China), all in analytical grade. Polystyrene 96-well and cell culture plates were provided by Corning Life Sciences (New York, USA). Eight to twelve-week-old female BALB/c mice were provided by Vital River Laboratory Animal Technology (Beijing, China). All the animal experiments were performed in compliance with the guidance of the Animal Ethics Committee of China Agricultural University (Aw32602202-2-2). Buffer solutions used in this study, including coating

Mari *et al. One Health Advances* (2023) 1:6

Page 9 of 12

buffer, washing buffer, blocking buffer, antibody dilution buffer, substrate solution and stop buffer solutions are mentioned in the *Supporting Information*.

Haptens synthesis and characterization

Two haptens were designed, and the synthetic routes are described in Scheme 1. Nitrophenyl derivatived OXZ (NPOXZ) was also synthesized for specificity characterization of antibodies. The chemical structures of the obtained haptens and NPOXZ were confirmed by mass spectrometry (Agilent Technologies, CA, USA) and nuclear magnetic resonance (NMR) DRX (Bruker, Rheinstetten, Germany), with the identified data presented in Figure S1 and S2 of the *Supporting Information*.

Hapten A was synthesized as follows: 5-hydroxy-2-nitrobenzaldehyde (compound 1) and ethyl 4-bromobutanoate at 1.0 mmol each and potassium carbonate at 2.0 mmol were mixed and acetonitrile was employed as the solvent. A small amount of potassium iodide was added as the catalyst and the mixtures were refluxed for reaction overnight at room temperature as shown in Step 1. Then the acetonitrile was removed by evaporation and precipitates were treated with distilled water. The resulting mixtures were extracted with ethyl acetate three times and combined, then washed, dried, and spin-dried to get compound 2 as shown in Scheme 1 (yield, 60%). In Step 2, 1.0 mmol of the attained compound 2 in methanol was reacted with 3.0 mmol sodium hydrate solution at 30℃ for 2 h. Hydrochloric acid (6 M) was added to adjust the pH value into an acidic state where the mixture solution was precipitated, and finally get yellow powder product (compound 3, yield, 80%) by suction filtration and drying under vacuum conditions. Followed by, compound 3 and OXZ at 1.0 mmol each were dissolved in ethanol to be refluxed under vigorous stirring for 3 h in Step 3. The mixtures were cooled at room temperature, and then obtained mixtures were cleaned and dried to acquire the yellowish powder (Hapten A, yield, 90%). HRMS (m/z)

in Step 1. HRMS (m/z) calc. for $C_{11}H_{10}N_4O_7$, 310.05, found 311.11 $[M+H]^+$; ^1H NMR (400 MHz, DMSO-d6) δ 12.49 (s, 1H, NH), 9.02 (s, 1H, CHO), 8.29 (s, 1H, NH_2), 8.10 (d, J=9.1 Hz, 1H, ArH), 7.96 (s, 1H, NH_2), 7.37 (d, J=2.6 Hz, 1H, ArH), 7.18 (d, J=9.1, 2.6 Hz, 1H, ArH), 4.88 (s, 2H, CH_2).

NPOXZ. The *o*-nitrophenyl formaldehyde (compound 6) and OXZ at 1.0 mmol each were added in anhydrous ethanol, after which the solution was allowed to react for 2 h and the mixture was cooled at room temperature. The filtrates underwent vacuum drying and yellowish powder (NPOXZ, yield, 90%) was obtained. HRMS (m/z) calc. for $C_9H_8N_4O_4$, 236.05, found 237.06 $[M+H]^+$; ^1H NMR (400 MHz, DMSO-d6): δ 12.47 (s, 1H, NH), 8.95 (s, 1H, CHO), 8.30 (s, 1H, NH_2), 8.05 (d, J=8.2 Hz, 1H, ArH), 8.02 (d, J=7.9 Hz, 1H, ArH), 7.96 (s, 1H, NH_2), 7.79 (t, J=7.6 Hz, 1H, ArH), 7.67 (t, J=7.8 Hz, 1H, ArH).

Synthesis of immunogens and coating antigens

Two haptens were conjugated to KLH and BSA using the active ester method according to previous work with some modifications [31]. In the first step, each hapten (0.1 mmol), NHS (0.15 mmol) and DCC (0.1 mmol) were mixed and dissolved in 0.5 mL DMF. The resulting mixture was gently stirred at 4℃ for 5 h to activate the carboxylic acid. The reacted solution was then separated into two portions and added drop-wise to separate solutions of BSA (20 mg BSA in 9.5 mL of PBS) and KLH (20 mg KLH in 9.5 mL PBS), respectively. The resultant solutions were left on a stirrer overnight, and the conjugate solutions were collected after dialysis in PBS for 48 h at 4℃. The BSA conjugates were evaluated using matrix-assisted laser desorption ionization time-of-flight mass spectrometry (MALDI-TOF–MS) (Bruker, Rheinstetten, Germany) . The molar coupling ratios were calculated using Eq. 1. The hapten-KLH conjugates were used as immunogens and stored at -70℃, while hapten-BSA conjugates were stored at -20℃ before use as coating antigens.

$$\text{Molar coupling ratio} = (\text{MW}_{\text{conjugate}} - \text{MW}_{\text{BSA}})/\text{MW}_{\text{hapten}} \quad (1)$$

calc. for $C_{13}H_{14}N_4O_7$, 338.09, found 339.09 $[M+H]^{+1}$; ^1H NMR (400 MHz, DMSO-d6) δ 12.49 (s, 1H, NH), 9.03 (s, 1H, CHO), 8.28 (s, 1H, NH_2), 8.11 (d, J=9.1 Hz, 1H, ArH), 7.96 (s, 1H, NH_2), 7.36 (d, J=2.5 Hz, 1H, ArH), 7.19 (d, J=9.1, 2.5 Hz, 1H, ArH), 4.14 (t, J=6.3 Hz, 2H, CH_2), 2.38 (t, J=7.2 Hz, 2H, CH_2), 2.03 – 1.87 (m, 2H, CH_2).

Hapten B. The synthesis process of Hapten B was similar to that of Hapten A as revealed in Scheme 1. In short, Hapten B (yield, 90%) was synthesized by ethyl 2-bromoacetate instead of ethyl 4-bromobutanoate as shown

Conformational and electronic analysis of haptens and analytes

To investigate the rationality of the hapten design, three-dimensional structures of haptens, NPOXZ, OXZ and NAZ were generated using GaussView 5.0 software (Gaussian, Wallingford, CT, USA). The haptens and analytes were then optimized using calculations based on M06-2X density functional theory with the TZVP basis set in the Gaussian 09 package (Gaussian, Wallingford, CT, USA), and atom charges were extracted directly from the Gaussian output files. Molecular electrostatic

Mari *et al. One Health Advances*   (2023) 1:6

Page 10 of 12

potential surfaces (ESP) were analyzed using the Gaussian 09 and GaussView 5.0 packages. Molecule alignment under the lowest-energy conformation was achieved in Discovery Studio 2019 (Accelrys Software, Inc., San Diego, CA, USA).

Production of mAbs

Ten female BALB/c mice (8 weeks old) were divided into two separate groups and subcutaneously immunized with either Hapten A-KLH or Hapten B-KLH. For the first immunization, 100 μg of the immunogens in 0.9% NaCl were emulsified with Freund's complete adjuvant (FCA) in equal volume, to form water-in-oil. Booster immunizations were executed with Freund's incomplete adjuvant instead of FCA [32], and each injection was administered at three week intervals [33]. After the third immunization, which was given seven days before collection, the antisera were obtained from the eye socket vein and the antibody titer and affinity (represented by IC_{50} of icELISA) were assessed using icELISA. The optical density (OD) was measured using a multimode plate reader (Waltham MA, USA). Finally, the mice selected as spleen donors for hybridoma production received a booster dose of intraperitoneal injection with 300 μg immunogen mixed with 0.9% NaCl. Three days later, the spleen cells of mice were fused with pre-resuscitated SP2/0 myeloma cells [34]. Fused cells were screened using culture in hypoxanthine aminopterin thymidine (HAT) for approximately seven days. The cell culture supernatants were then assayed for titer and inhibition ratios by icELISA. Positive hybridomas with high affinity were cloned by limiting dilution to obtain a single cell. Some of the hybridomas were cryopreserved in liquid nitrogen, while others were cultured, and then injected intraperitoneally into adult female BALB/c mice to generate a large volume of ascites. The ascites were stored at -20°C for later use [35].

Establishment and Optimization of icELISA

Polystyrene plates were coated with (100 μL well^{-1}) coating antigen Hapten A-BSA or Hapten B-BSA in coating buffer (pH 9.6) and incubated at 37°C for 2 h. After incubation, the plates were washed three times with washing buffer (see *Supporting Information*), and the unoccupied sites were blocked by adding blocking buffer (150 μL well^{-1}). The plates were then incubated at 37°C for 1 h [36, 37]. Subsequently, 50 μL of OXZ (or other competitors) standard solutions and the same quantity of antibody solution, were added to the polystyrene plates in sequence and incubated for 30 min at 37°C followed by washing three times. HRP labeled goat anti-mouse IgG

at a 5000-fold dilution (100 μL well^{-1}) was then added, and the plates were incubated for 30 min at 37°C. Subsequently, the plates were washed four times, and a mixed substrate solution (100 μL well^{-1}) was added to give color, the plates were then incubated at 37°C for 15min. In the final step, 50 μL well^{-1} of stop buffer (H_2SO_4) was added, and the values of OD at 450 nm were read immediately. The standard curve was generated using a four-parameter logistic regression model, which is described in the following Eq. 2.

$$Y = (A - B)/[1 + (X/C)^D] + B \tag{2}$$

Where X is the concentration of the analytes. A is the response at the up asymptote of the curve, B is the response at the down asymptote, C is the concentration of the analytes corresponding to 50% inhibition (IC_{50}), and D is the gradient factor at the increasing area of the sigmoid.

To characterize the specificity of antibodies, cross-reactivity (CR) was assessed with a series of analogues, including other nitrofurans and metabolite derivatives. CR was analyzed based on the following Eq. 3:

$$CR = IC_{50} \text{ of } OXZ/(IC_{50} \text{ of analogues}) \times 100\% \tag{3}$$

To improve the sensitivity of the icELISA, the effects of physicochemical parameters, such as temperature, pH, and ionic strength, were further studied. The consequences of these factors, i.e., A_{max} (the absorbance value of analyte concentration at zero) and IC_{50} values were used as quantitative criteria.

Matrix effect and recovery analysis

After homogenization, 1.0 g of chicken sample was placed in a centrifuge tube, and fortified with OXZ standard solutions at the final levels of 0.5, 1.0 and 2.5 μg kg^{-1} separately. The extraction procedure of OXZ from samples was based on a previous report [17]. Briefly, samples were dunked into the mixed solution of 0.5 mL hydrochloric acid (1.0 mM) and 4.0 mL deionized water before ultra-sonication for 20 min and kept in the water bath at 60°C for 30 min to release the bound OXZ from the tissue proteins. Next, 5.0 mL of di-potassium phosphate at a concentration of 0.1 mM was added, followed by 0.4 mL of sodium hydrate (1.0 mM) to adjust pH value to 7.0. Subsequently, 6.0 mL of ethyl acetate, was added, and the mixture was vortexed for 10 min before being allowed to centrifuge at 5000 g for 10 min. Finally, 3.0 mL of the upper organic phase was separated and dehydrated under a nitrogen flow at 55°C, afterwards a re-diluent of dried residues sample in n-hexane and PBS at 1.0 mL each was centrifuged for 5 min at 5000 g, then lower phase of the solution was collected for icELISA detection.

Mari *et al. One Health Advances*   (2023) 1:6

Page 11 of 12

The limit of detection (LOD) was defined as the concentration corresponding to the average absorbance value of 20 blank samples plus three times the standard deviation. A total of 15 spiked chicken samples were pretreated as above for recovery studies, in order to evaluate accuracy and precision of the developed icELISA. And recovery was analyzed according to Eq. 4 as described below:

$$\text{Recovery (\%)} = (\text{assessed values } (\mu g \, kg^{-1})/ \text{ spiked values } (\mu g \, kg^{-1})) \times 100\% \tag{4}$$

Supplementary Information

The online version contains supplementary material available at https://doi.org/10.1186/s44280-023-00006-y.

Additional file 1.

Authors' contributions

G.M.M. designed, performed the experiments, and wrote the original draft. W.L.W. provided data curation, visualization and revised the manuscript. A.T., J.M.S. and S.A. provided investigation and methodology. F.K., E.B. and A.S. performed review and editing. Z.H.W. provided methodology, funding acquisition and project administration. S.A.E. provided conceptualization, supervision, and writing. All authors have read and approved the final manuscript.

Declarations

Ethics approval and consent to participate

Animal care and all animal experiments were performed in compliance with the Guidance for the Care and Use of Laboratory Animals produced by the China Agricultural University. The study was approved by the Animal Ethics Committee of China Agricultural University (Aw32602202-2-2).

Competing interests

The authors stated that they have no conflict of financial interest.

References

1. Radovnikovic A, Moloney M, Byrne P, Danaher M. Detection of banned nitrofuran metabolites in animal plasma samples using UHPLC–MS/MS. J Chromatogr B. 2011;879:159–66.
2. Khong SP, Gremaud E, Richoz J, Delatour T, Guy PA, Stadler RH, et al. Analysis of matrix-bound nitrofuran residues in worldwide-originated honeys by isotope dilution high-performance liquid chromatography-tandem mass spectrometry. J Agric Food Chem. 2004;52:5309–15.
3. Commission Regulation (EC) 1442/95 of 26 June 1995 amending Council Regulation (ECC) No 2377/90 laying down a Community Procedure for the establishment of maximum residue limits of veterinary medicinal products in foodstuffs of animal origin. Off J Eur Communities. 1995;L143:26–30.
4. Decision C. 2003/181/EC of 13 March 2003 amending Decision 2002/657/EC as regards the setting of minimum required performance limits (MRPLs) for certain residues in food of animal origin. Off J Eur Communities. 2003;L071:17–8.
5. Commission Regulation 2019/1871 of 7 November 2019 on reference points for action for non-allowed pharmacologically active substances present in food of animal origin and repealing Decision 2005/34/EC (Text with EEA relevance). Off J Eur Communities. 2019;L289:41–46.
6. Nouws JF, Laurensen J. Postmortal degradation of furazolidone and furaltadone in edible tissues of calves. Vet Q. 1990;12:56–9.
7. McCracken RJ, Blanchflower WJ, Rowan C, Mccoy MA, Kennedy DG. Determination of furazolidone in porcine tissue using thermospray liquid chromatography-mass spectrometry and a study of the pharmacokinetics and stability of its residues. Analyst. 1995;120:2347–51.
8. Zuidema T, van Rhijn JA, Schat B, Mulder PPJ, Bolck YJC, Hoogen-boom LAP, et al. Metabolism and depletion of furazolidone and furaltadone in broilers. Proceedings of the EuroResidue Conference V; 2004 May 10–12; Noordwijkerhout, The Netherlands; 2004. p. 996–1001.
9. Cooper KM, Mulder PP, van Rhijn JA, Kovacsics L, McCracken RJ, Young PB, et al. Depletion of four nitrofurans antibiotics and their tissue-bound metabolites in procine tissues and determination using LC-MS/MS and HPLC-UV. Food Addit Contam. 2005;22:406–14.
10. McCracken RJ, Kennedy DG. The bioavailability of residues of the furazolidone metabolite 3-amino-2-oxazolidinone in porcine tissues and the effect of cooking upon residue concentrations. Food Addit Contam. 1997;14:507–13.
11. Liu X, Xia F, Zhang S, Cheng Y, Fan L, Kang S, et al. Dual-color aggregation-induced emission nanoparticles for simultaneous lateral flow immunoassay of nitrofuran metabolites in aquatic products. Food Chem. 2023;402:134235.
12. Cheng Y, Liu X, Yang M, Xia F, Fan L, Gao X, et al. Ratiometric fluorescent immunochromatography for simultaneously detection of two nitrofuran metabolites in seafoods. Food Chem. 2023;404:134698.
13. Ding X, Liu L, Song S, Kuang H, Xu C. Rapid and ultrasensitive detection of 3-amino-2-oxazolidinone in catfish muscle with indirect competitive enzyme-linked immunosorbent and immunochromatographic assays. Food Agric Immunol. 2017;28:463–75.
14. Melekhin AO, Tolmacheva VV, Kholyavskaya YN, Sedykh ES, Dmitrienko SG, Apyari VV, et al. Rapid hydrolysis and derivatization of nitrofuran metabolites with a new derivatizing agent 5-nitro-2-furaldehyde in their determination in chicken meat by HPLC–MS/MS. J Anal Chem. 2022;77:1300–6.
15. Yang M, Yi J, Wei C, Lu Y, Yang Y, Yang Z, et al. Rapid determination of nitrofuran metabolites residues in honey by ultrasonic assisted derivatization-QuEChERS-high performance liquid chromatography/tandem mass spectrometry. J Food Compos Anal. 2022;114:104812.
16. Melekhin AO, Tolmacheva VV, Shubina EG, Dmitrienko SG, Apyari VV, Grudev AI. Determination of nitrofuran metabolites in honey using a new derivatization reagent, magnetic solid-phase extraction and LC–MS/MS. Talanta. 2021;230:122310.
17. Song J, Yang H, Wang Y, Si W, Deng A. Direct detection of 3-amino-5-methylmorpholino-2-oxazolidinone (AMOZ) in food samples without derivatisation step by a sensitive and specific monoclonal antibody based ELISA. Food Chem. 2012;135:1330–6.
18. Mari GM, Li H, Dong B, Yang H, Talpur A, Mi J, et al. Hapten synthesis, monoclonal antibody production and immunoassay development for direct detection of 4-hydroxybenzehydrazide in chicken, the metabolite of nifuroxazide. Food Chem. 2021;355:129598.
19. Register F. Topical nitrofurans, extralabel animal drug use, order of prohibition. Fed Reg. 2002;67:5470–1.
20. Ministry of Agriculture and Rural Affairs of the People's Republic of China. The banned list of veterinary medicine and other compounds for food-producing animals. 2020, No. 250.
21. Shen YD, Xu ZL, Zhang SW, Wang H, Yang JY, Lei HT, et al. Development of a monoclonal antibody-based competitive indirect enzyme-linked immunosorbent assay for furaltadone metabolite AMOZ in fish and shrimp samples. J Agric Food Chem. 2012;60:10991–7.
22. Regan G, Moloney M, Di Rocco M, McLoughlin P, Smyth W, Crooks S, et al. Development and validation of a rapid LC–MS/MS method for the confirmatory analysis of the bound residues of eight nitrofuran drugs in meat using microwave reaction. Anal Bioanal Chem. 2022;414:1375–88.
23. Regan, G. Analysis of nitrofuran drug residues in animal tissues using liquid chromatography coupled to tandem mass spectrometry[dissertation]. Belfast: Queen's University Belfast; 2023.

Mari *et al. One Health Advances*   (2023) 1:6

Page 12 of 12

24. Wu W, Yang S, Liu J, Mi J, Dou L, Pan Y, et al. Progress in immunoassays for nitrofurans detection. Food Agric Immunol. 2020;31:907–26.
25. Maximilian R, Anja HR. Antibody recognition of fluorinated haptens and antigens. Curr Top Med Chem. 2014;14:840–54.
26. Wang Z, Beier RC, Shen J. Immunoassays for the detection of macrocyclic lactones in food matrices–a review. Trends Anal Chem. 2017;92:42–61.
27. Vasylieva N, Barnych B, Rand A, Inceoglu B, Gee SJ, Hammock BD. Sensitive immunoassay for detection and quantification of the neurotoxin, tetramethylenedisulfotetramine. Anal Chem. 2017;89:5612–9.
28. Song J, Wang RM, Wang YQ, Tang YR, Deng AP. Hapten design, modification and preparation of artificial antigens. Chinese J Anal Chem. 2010;38:1211–8.
29. Xu L, Peng S, Liu L, Song S, Kuang H, Xu C. Development of sensitive and fast immunoassays for amantadine detection. Food Agric Immunol. 2016;27:678–88.
30. Liang X, Ni H, Beier RC, Dong Y, Li J, Luo X, et al. Highly broad-specific and sensitive enzyme-linked immunosorbent assay for screening of the sulfonamides: assay optimization and application to milk samples. Food Anal Methods. 2014;7:1992–2002.
31. Wang Z, Li N, Zhang S, Zhang H, Sheng Y, Shen J. Production of antibodies and development of enzyme-linked immunosorbent assay for valnemulin in porcine liver. Food Addit Contam, Part A. 2013;30:244–52.
32. Wang Z, Wen K, Zhang X, Li X, Shen J, Ding S. New hapten synthesis, antibody production, and indirect competitive enzyme-linked immnunosorbent assay for amantadine in chicken muscle. Food Anal Methods. 2018;11:302–8.
33. Guan D, Guo L, Liu L, Kong N, Kuang H, Xu C. Development of an ELISA for nitrazepam based on a monoclonal antibody. Food Agric Immunol. 2015;26:611–21.
34. Wang Z, Mi T, Beier RC, Zhang H, Sheng Y, Shi W, et al. Hapten synthesis, monoclonal antibody production and development of a competitive indirect enzyme–linked immunosorbent assay for erythromycin in milk. Food Chem. 2015;171:98–107.
35. Zhang X, Wen K, Wang Z, Jiang H, Beier RC, Shen J. An ultra-sensitive monoclonal antibody-based fluorescent microsphere immunochromatographic test strip assay for detecting aflatoxin M1 in milk. Food Control. 2016;60:588–95.
36. Chen G, Huang X, Li S, Kong X, Huai B. Synthesis of a newly designed artificial antigen and preparation of a polyclonal antibody against salbutamol. Food Agric Immunol. 2014;25:322–31.
37. Suryoprabowo S, Liu L, Peng J, Kuang H, Xu C. Development of a broad specific monoclonal antibody for fluoroquinolone analysis. Food Anal Methods. 2014;7:2163–8.

Publisher's Note